An ab Initio/RRKM Study of Product Branching Ratios in the Photodissociation of Buta-1,2- and -1,3-dienes and But-2-yne at 193 nm

Hwa-Yu Lee,[a] Vadim V. Kislov,[a,b] Sheng-Hsien Lin,[a] Alexander M. Mebel,*[a] and Daniel M. Neumark[c]

Abstract: Ab initio G2M(MP2)//B3LYP/6-311G** calculations have been performed to investigate the reaction mechanism of photodissociation of buta-1,2- and -1,3-dienes and but-2-yne after their internal conversion into the vibrationally hot ground electronic state. The detailed study of the potential-energy surface was followed by microcanonical RRKM calculations of energy-dependent rate constants for individual reaction steps (at 193 nm photoexcitation and under collision-free conditions) and by solution of kinetic equations aimed at predicting the product branching ratios. For buta-1,2-diene, the major dissociation channels are found to be the single C–C bond cleavage to form the methyl and propargyl radicals and loss of hydrogen atoms from various positions to produce the but-2-yn-1-yl (**p1**), buta-1,2-dien-4-yl (**p2**), and but-1-yn-3-yl (**p3**) isomers of C_4H_5. The calculated branching ratio of the $CH_3 + C_3H_3/C_4H_5 + H$ products, 87.9:5.9, is in a good agreement with the recent experimental value of 96:4 (ref. [21]) taking into account that a significant amount of the C_4H_5 product undergoes secondary dissociation to $C_4H_4 + H$. The isomerization of buta-1,2-diene to buta-1,3-diene or but-2-yne appears to be slower than its one-step decomposition and plays only a minor role. On the other hand, the buta-1,3-diene → buta-1,2-diene, buta-1,3-diene → but-2-yne, and buta-1,3-diene → cyclobutene rearrangements are significant in the dissociation of buta-1,3-diene, which is shown to be a more complex process. The major reaction products are still $CH_3 + C_3H_3$, formed after the isomerization of buta-1,3-diene to buta-1,2-diene, but the contribution of the other radical channels, $C_4H_5 + H$ and $C_2H_3 + C_2H_3$, as well as two molecular channels, $C_2H_2 + C_2H_4$ and $C_4H_4 + H_2$, significantly increases. The overall calculated $C_4H_5 + H/CH_3 + C_3H_3/C_2H_3 + C_2H_3/C_4H_4 + H_2/C_2H_2 + C_2H_4$ branching ratio is 24.0:49.6:4.6:6.1:15.2, which agrees with the experimental value of 20:50:8:2:20[22] within 5% margins. For but-2-yne, the one-step decomposition pathways, which include mostly H atom loss to produce **p1** and, to a minor extent, molecular hydrogen elimination to yield methylethynylcarbene, play an approximately even role with that of the channels that involve the isomerization of but-2-yne to buta-1,2- or -1,3-dienes. **p1** + H are the most important reaction products, with a branching ratio of 56.6%, followed by $CH_3 + C_3H_3$ (23.8%). The overall $C_4H_5 + H/CH_3 + C_3H_3/C_2H_3 + C_2H_3/C_4H_4 + H_2/C_2H_2 + C_2H_4$ branching ratio is predicted as 62.0:23.8:2.5:5.7:5.6. Contrary to buta-1,2- and -1,3-dienes, photodissociation of but-2-yne is expected to produce more hydrogen atoms than methyl radicals. The isomerization mechanisms between various isomers of the C_4H_6 molecule including buta-1,2- and -1,3-dienes, but-2-yne, 1-methylcyclopropene, dimethylvinylidene, and cyclobutene have been also characterized in detail.

Keywords: ab initio calculations · butadiene · kinetics · photolysis · product branching ratios

Introduction

The primary photochemistry of unsaturated hydrocarbons is a subject of great interest for experimentalists and theorists because, upon UV excitation of these species, multiple product channels are energetically accessible and numerous products can be formed in various isomeric forms.[1] Photodissociation experiments provide information on important dynamical issues, such as energy disposal by excited molecules and radicals, the extent to which isomerization occurs before decomposition of the excited molecule, and whether dissociation takes place on an excited or the ground electronic state

[a] Dr. A. M. Mebel, Dr. H. Y. Lee, Dr. V. V. Kislov, Prof. S. H. Lin
Institute of Atomic and Molecular Sciences, Academia Sinica
P.O. Box 23-166, Taipei 10764 (Taiwan)
Fax: (+886) 2-23620200
E-mail: mebel@po.iams.sinica.edu.tw

[b] Permanent address: Institute of Solution Chemistry
Russian Academy of Sciences
Akademicheskaya St. 1
Ivanova 153045 (Russia)

[c] Prof. D. M. Neumark
Chemical Science Division
Lawrence Berkeley National Laboratory and Department of Chemistry
University of California, Berkeley, California 94720 (USA)

0947-6539/03/0903-0726 $ 20.00+.50/0

potential energy surface (PES). Meanwhile, accurate ab initio calculations of PESs for isomerization and dissociation pathways of unsaturated hydrocarbons are highly complimentary to the experimental studies of their photodissociation dynamics, because they give guidance on possible reaction products and their energies, and insight into various reaction mechanisms leading to these products. If a PES study is followed by Rice–Ramsperger–Kassel–Marcus (RRKM) calculations of rate constants for individual unimolecular reaction steps, relative product yields (branching ratios) can be predicted by assuming a complete energy randomization in the decomposing species. A comparison between the computed and measured branching ratios is informative for understanding the reaction dynamics, because it helps to clarify whether the system behaves statistically or nonstatistically, and to what extent excited electronic states can be involved in dissociation processes.

The unimolecular dissociation of buta-1,2- and -1,3-dienes has been investigated by using various experimental techniques including mercury photosensitization,[2] UV-visible photolysis,[3–11] and shock-tube pyrolysis.[12–20] The UV-visible photodissociation studies[3–11] showed that several reaction pathways can compete; these include methyl-radical loss, sequential atomic hydrogen loss, molecular hydrogen loss, acetylene loss, and methylene loss. The thermal decomposition of buta-1,2-diene gave mostly the $CH_3 + C_3H_3$ products, while the atomic hydrogen loss was insignificant. Additionally, isomerization of buta-1,2-diene to buta-1,3-diene, but-1-yne, and but-2-yne played an important role in the thermal studies.[13, 14] According to studies of the photodissociation of buta-1,3-diene at 213.8 nm,[9] the major fate of the photoexcited buta-1,3-diene molecule is isomerization to buta-1,2-diene followed by decomposition of the latter to methyl and C_3H_3 radicals (the major channel) and to acetylene + ethylene and vinylacetylene + H_2 (two minor channels). The above-mentioned studies were carried out at relatively high pressure; this means that multiple collisions can occur during the course of the measurement. This resulted in a possibility of collisional deactivation of various intermediates and secondary reactions of the primary products. On the other hand, recent photofragment translational spectroscopy studies of buta-1,2- and -1,3-dienes at 193 nm by Neumark and coworkers[21, 22] allowed them to look at the dissociation dynamics under collisionless conditions. The results indicated that the dissociation mostly occurs on the ground state PES after internal conversion of photoexcited molecules into vibrationally excited ground electronic state molecules. In such a case, theoretical modeling of photodissociation can be performed through a study of intermediates, transition states, and various products on the ground state surface followed by microcanonical RRKM calculations of unimolecular reaction-rate constants and product branching ratios.

In this work, we use high-level ab initio calculations to investigate reaction mechanisms for the isomerization of buta-1,2-diene to buta-1,3-diene and but-2-yne and for various decomposition channels of the three C_4H_6 isomers. To our knowledge, up to now, the buta-1,2-diene → buta-1,3-diene and buta-1,2-diene → but-2-yne rearrangements have been studied only at a moderate MP2/6-31G**/HF/6-31G** level,[23–25] and no theoretical data are available concerning the decomposition pathways. Molecular parameters and energies obtained by ab initio calculations are then employed in RRKM calculations of individual rate constants for various reaction steps, bearing in mind that the buta-1,2- and -1,3-diene and but-2-yne molecules are energized by a 193 nm photon (~ 148 kcal mol^{-1}). Product branching ratios are consequently obtained by solving kinetic equations, and the results are compared with the experimental relative product yields reported by Neumark and co-workers.[21, 22]

Computational Methods

Ab initio calculations: The geometries of the reactants, products, various intermediates, and transition states were optimized by using the hybrid density functional B3LYP/6-311G** method.[26, 27] Vibrational frequencies, calculated at the same level, were used for characterization of stationary points, zero-point-energy (*ZPE*) corrections, and RRKM calculations of reaction rate constants. All the stationary points were positively identified for minimum or transition state. In order to obtain more reliable energies, we used the G2M(CC,MP2) method,[28] a modification of the Gaussian-2 [G2(MP2)] approach.[29–32] The total energy in G2M is calculated as follows:[28]

$$E[\mathrm{G2M(CC,MP2)}] = E[\mathrm{CCSD(T)/6\text{-}311G^{**}}] + \Delta E(+\mathrm{3df2p}) + \Delta E(\mathrm{HLC}) + ZPE[\mathrm{B3LYP/6\text{-}311G^{**}}]$$

in which

$$\Delta E(+\mathrm{3df2p}) = E[\mathrm{MP2/6\text{-}311+G(3df,\,2p)}] - E[\mathrm{MP2/6\text{-}311G^{**}}]$$

In this study, we did not use the empirical "higher-level correction" (HLC) which depends on the numbers of paired and unpaired electrons in the molecule.[28] It should be noted that HLC would affect only the relative energies of radical products, increasing them by ~ 3 kcal mol^{-1}.

In order to scan the PES along the reaction coordinates corresponding to C–H or C–C bond cleavages for variational RRKM calculations, we used the unrestricted B3LYP method (UB3LYP) with the 6-311G** basis set. In this case, single point energies were recalculated by using the coupled cluster[33] UCCSD(T)/6-311G** method. The GAUSSIAN 98[34] and MOLPRO 2000[35] programs were employed for the ab initio calculations.

RRKM and variational transition state calculations: We used the RRKM theory for computations of rate constants of individual reaction steps.[36–38] Rate constant $k(E)$ at an internal energy E for a unimolecular reaction $A^* \rightarrow A^{\#} \rightarrow P$ can be expressed as:

$$k(E) = \frac{\sigma}{h} \cdot \frac{W^{\#}(E - E^{\#})}{\rho(E)}$$

in which σ is the symmetry factor, h is the Plank constant, $W^{\#}(E - E^{\#})$ denotes the total number of states for the transition state (activated complex) $A^{\#}$ with a barrier $E^{\#}$, $\rho(E)$ represents the density of states of the energized reactant molecule A*, and P is the product or products. It should be noted that we used the harmonic approximation to calculate the total number and density of states. For the case in which the excitation energy is large and low frequency modes exist, the harmonic approximation will not be accurate in calculating the total number and density of states and may introduce

  0947-6539/03/0903-0727 $ 20.00+.50/0

certain errors in our treatment. In order to take into account anharmonicity, more sophisticated RRKM calculations are required, but they are beyond the scope of the present work.

If no distinct transition state exists on the PES (as for the case of a simple bond-cleavage process), one can consider different positions for the transition state along the reaction path and calculate rate constants corresponding to each of them. The minimum rate so obtained is the closest to the truth, assuming that quantum effects related to tunneling and nonseparability are negligible. This procedure is called variational transition state theory (VTST).[36] In the microcanonical VTST, the minimum in the microcanonical rate constant is found along the reaction path according to the following equation:

$$\frac{dk(E)}{dq^{\#}} = 0$$

in which $q^{\#}$ is the reaction coordinate, such that a different transition state is found for each different energy. The individual microcanonical rate constants are minimized at the point along the reaction path where the sum of states $W^{\#}(E - E_0)$ has a minimum. Thus, the reaction bottleneck is located where the minimal sum of states is found, that is, the transition state's sum of states must be calculated along the reaction path. Each of these calculations requires values of the classical potential energy, zero-point energy, and vibrational frequencies as functions of the reaction coordinate.

We used the following procedure for the VTST calculations. First, we calculated a series of energies at different distances between two dissociating fragments corresponding to the length of a bond to be broken during dissociation; this is considered to be the reaction coordinate. To obtain these energies, we performed partial geometry optimization with fixed values of the reaction coordinate and all other geometric parameters being optimized. Then we calculated $3N-7$ vibrational frequencies projecting out the reaction coordinate. Finally, the variational transition states with the minimal values of the number of states were employed to calculate rate constants of the direct dissociation processes by using the above RRKM formalism.

Product branching ratios: Under collision-free molecular beam conditions, master equations for unimolecular reactions can be expressed as follows:

$$\frac{d[C]_i}{dt} = \Sigma k_n[C]_j - \Sigma k_m[C]_i$$

in which $[C]_i$ and $[C]_j$ are concentrations of various intermediates or products, k_n and k_m are microcanonical rate constants computed as described in the previous subsection. The fourth-order Runge–Kutta method[36–38] was used to solve the system of the master equations. We obtained numerical solutions for concentrations of various products versus time. The concentrations at the times when they have converged were used for calculations of product branching ratios. Additionally, we used the steady-state approximation to compute the branching ratios and nearly identical results were obtained.

Results and Discussion

Potential energy surface: The optimized geometries of various intermediates, transition states, and products are presented in Figures 1–3, while the calculated profile of the PESs for isomerization of the three C_4H_6 isomers and their decomposition pathways is shown in Figure 4. Relative energies of various species calculated at the B3LYP/6-311G**, MP2/6-311G**, CCSD(T)/6-311G**, MP2/6-311+G(3df,2p), and G2M levels of theory are collected in Table 1 and their B3LYP/6-311G** vibrational frequencies are shown in Table 2.

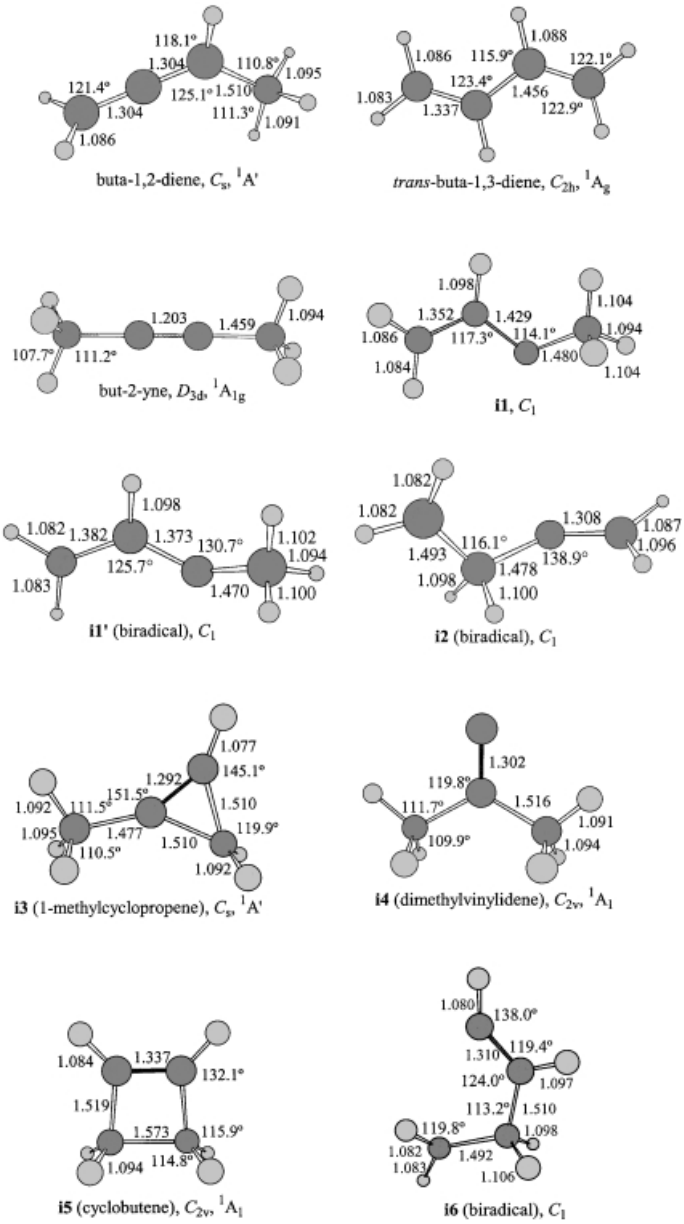

Figure 1. B3LYP/6-311G**-optimized geometries of the reactants and reaction intermediates in the photodissociation of buta-1,2- and -1,3-dienes and but-2-yne. (Bond lengths are given in Å and bond angles are in degrees).

0947-6539/03/0903-0728 $ 20.00+.50/0 *Chem. Eur. J.* **2003**, *9*, No. 3

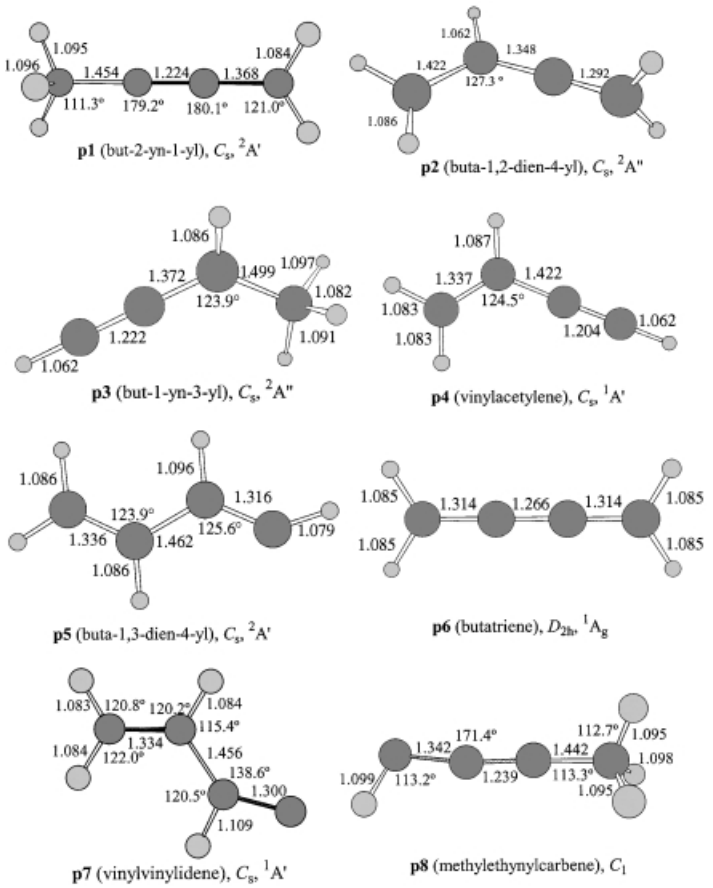

Figure 2. B3LYP/6-311G**-optimized geometries of various reaction products in the photodissociation of buta-1,2- and -1,3-dienes and but-2-yne. (Bond lengths are given in Å and bond angles are in degrees).

Decomposition of buta-1,2-diene: The most energetically favorable pathway for decomposition of buta-1,2-diene is a cleavage of the single C–C bond leading to the methyl (CH_3) and propargyl (C_3H_3) radical products. This reaction occurs without an exit barrier, and the C–C bond strength calculated at the CCSD(T)/6-311G** and G2M levels of theory is 76.1 and 77.8 kcal mol^{-1}, respectively. Both values are in close agreement with the experimental endothermicity of the C_4H_6 (buta-1,2-diene) $\rightarrow CH_3 + C_3H_3$ reaction, 77.0 kcal mol^{-1}, obtained based on the enthalpies of formation taken from the NIST Thermochemical Database.[39] Three distinct products can be formed by elimination of a hydrogen atom from buta-1,2-diene. First, H loss from the secondary C–H bond gives the but-2-yn-1-yl isomer of the C_4H_5 radical (**p1**) with an energy loss of 85.1 kcal mol^{-1}. Second, the elimination of a methyl H atom produces buta-1,2-dien-4-yl (**p2**) with an endothermicity of 86.9 kcal mol^{-1}, and finally, the C–H bond fission on the terminal CH_2 group yields but-1-yn-3-yl (**p3**) with an energy loss of 87.4 kcal mol^{-1}. At the G2M level, the buta-1,2-dien-4-yl and but-1-yn-3-yl isomers of C_4H_5 lie 1.8 and 2.3 kcal mol^{-1} higher in energy than but-2-yn-1-yl. Interestingly, at the CCSD(T)/6-311G** level, the relative energetic order of **p2** and **p3** is different; they reside 2.3 and 1.9 kcal mol^{-1}, respectively, above **p1** (see Table 1). Similar values were obtained in earlier QCISD and CCSD(T) calculations by Parker and Cooksy.[40] However, the basis-set correction in the

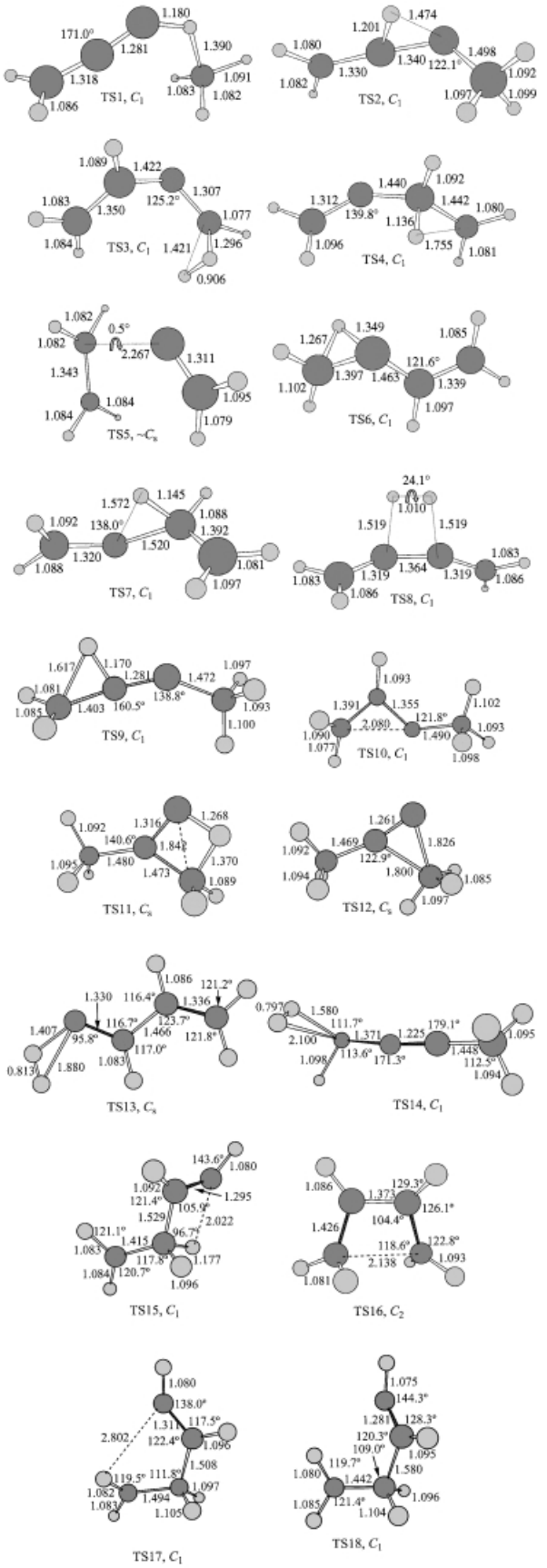

Figure 3. B3LYP/6-311G**-optimized geometries of transition states for various isomerization and fragmentation pathways of buta-1,2- and -1,3-dienes and but-2-yne. (Bond lengths are given in Å and bond angles are in degrees).

  0947-6539/03/0903-0729 $ 20.00+.50/0

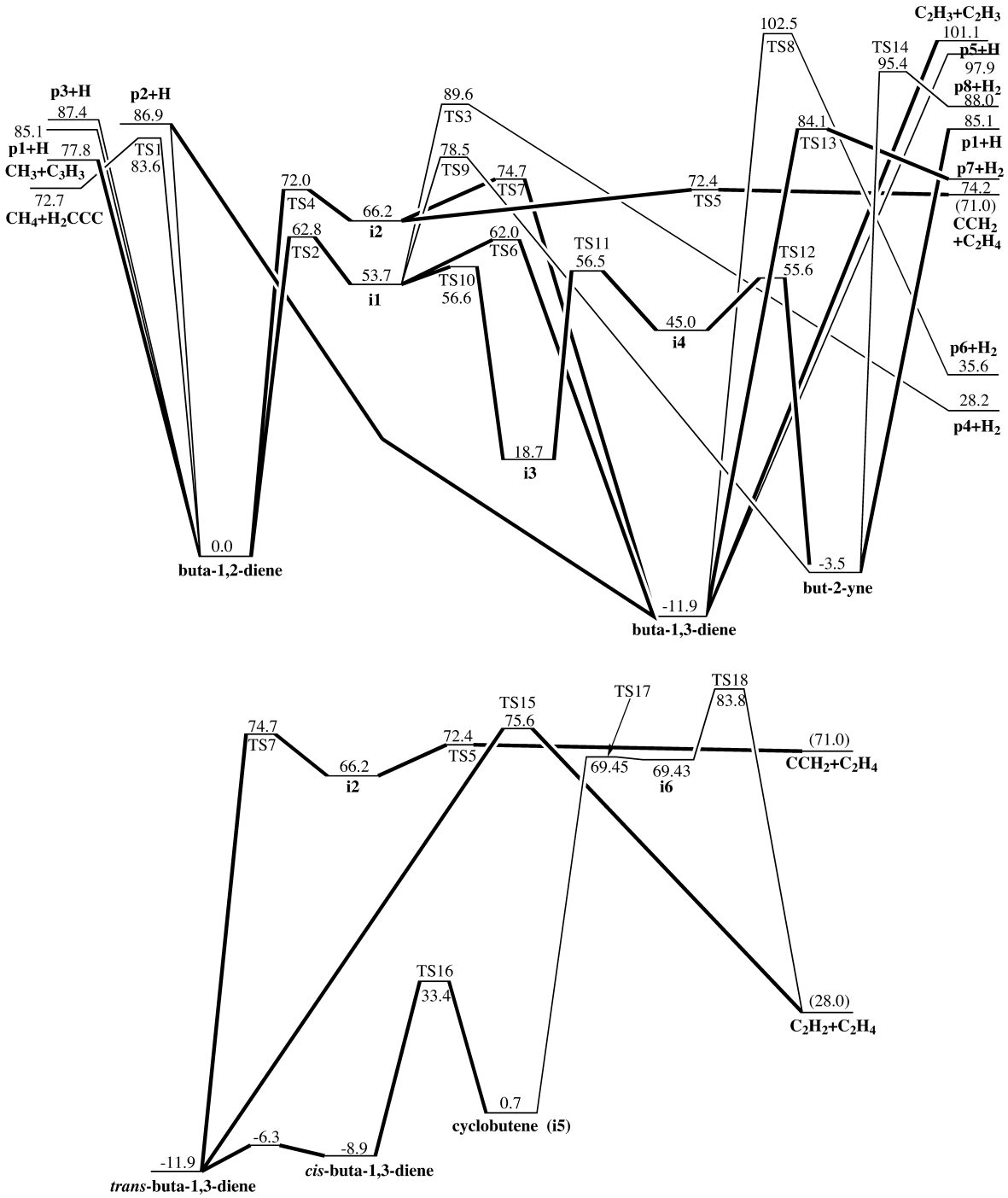

Figure 4. Potential energy diagram for various isomerization and fragmentation pathways of buta-1,2- and -1,3-dienes and but-2-yne calculated at the G2M level. Energies of various species are given in kcal mol^{-1}. The lower panel shows pathways related to the dissociation of buta-1,3-diene to the $C_2H_2 + C_2H_4$ products. Bold lines show the most important reaction channels.

G2M scheme makes buta-1,2-dien-4-yl slightly more stable than but-1-yn-3-yl. We can conclude here that the **p2** and **p3** isomers of the C_4H_5 radical are very close in energy and lie about 2 kcal mol^{-1} higher in energy than the most stable but-2-yn-1-yl structure.

Neumark and co-workers[21] suggested that the C_4H_5 products of the primary photodissociation of buta-1,2-diene can undergo secondary decomposition if their internal energy is sufficiently high. A detailed description of the isomerization and decomposition pathways on the C_4H_5 PES in relation to the reaction of atomic carbon, $C(^3P)$, with the allyl radical, C_3H_6, will be the subject of a subsequent paper.[41] Let us mention here only the most favorable channels for dissociation of the but-2-yn-1-yl, buta-1,2-dien-4-yl, and but-1-yn-3-yl isomers. But-2-yn-1-yl can lose a methyl hydrogen to produce butatriene, H_2CCCCH_2, with an endothermicity of 52.5 kcal mol^{-1} over a barrier of 63.2 kcal mol^{-1}. However, the barrier for the but-2-yn-1-yl → buta-1,2-dien-4-yl rearrangement by a 1,2-H shift is lower, 55.7 kcal mol^{-1}, and buta-1,2-dien-4-yl dissociates to vinylacetylene + H with a barrier of

0947-6539/03/0903-0730 $ 20.00+.50/0 *Chem. Eur. J.* **2003**, *9*, No. 3

Table 1. Zero-point energies (*ZPE*) calculated at the B3LYP/6-311G** level and relative energies [kcal mol^{-1}] of reactants, intermediates, transition states, and products in the photodissociation of buta-1,2-diene, buta-1,3-diene, and but-2-yne obtained at the B3LYP/6-311G**, MP2/6-311G**, CCSD(T)/6-311G**, MP2/6-311 + G(3df,2p), and G2M levels.

Species	*ZPE*	B3LYP/ 6-311G**	MP2/ 6-311G**	CCSD(T)/ 6-311G**	MP2/ 6-311 + G(3df,2p)	G2M
buta-1,2-diene	52.45	0.0	0.0	0.0	0.0	0.0
buta-1,3-diene	53.21	−10.00	−11.22	−11.31	−11.81	−11.90 (−12.8)[a]
but−2−yne	52.56	−2.12	−7.54	−3.90	−7.14	−3.50 (−4.1)[a]
i1	50.95	54.11	57.42	53.53	57.54	53.65
i1′ (biradical)	50.22	50.71	62.61	52.93	63.97	54.29
i2 (biradical)	49.28	64.56	71.99	64.30	73.92	66.23
i3	52.72	21.36	14.76	18.09	15.36	18.69
i4	51.78	48.70	47.87	43.49	49.38	45.00
i5 (cyclobutene)	54.03	5.07	−2.31	−0.18	−1.42	0.70 (−1.3)[a]
i6 (biradical)	49.52	68.72	75.51	67.18	77.76	69.43
TS1	47.53	82.44	87.34	84.24	86.71	83.61
TS2	49.01	61.49	65.15	64.16	63.82	62.83
TS3	46.59	88.62	94.02	91.99	91.61	89.58
TS4	48.93	81.75	79.12	74.02	77.13	72.03
TS5	49.31	73.21	77.56	72.14	77.84	72.42
TS6	49.40	63.61	64.05	62.85	63.16	61.97
TS7	49.27	80.07	79.36	76.68	77.37	74.69
TS8	44.64	101.22	105.18	104.19	103.52	102.53
TS9	48.62	78.60	83.10	80.57	81.05	78.52
TS10	50.77	57.28	59.66	56.79	59.45	56.58
TS11	50.00	60.74	54.22	55.96	54.75	56.49
TS12	50.99	59.53	54.29	55.29	54.60	55.60
TS13	46.33	84.89	89.99	84.80	89.28	84.09
TS14	45.02	90.61	97.29	95.69	96.98	95.38
TS15	48.35	93.38	83.17	76.77	82.01	75.61
TS16	52.37	37.30	31.42	33.60	31.17	33.35
TS17 (biradical)	49.49	68.70	75.65	67.18	77.92	69.45
TS18	49.36	92.76	89.53	(85.09)[b]	88.27	(83.83)[c]
p1 + H	43.55	82.79	86.82	83.74	88.19	85.11
p2 + H	43.87	84.52	94.34	86.03	95.19	86.87
p3 + H	43.70	86.55	90.11	85.66	91.82	87.38
p4 + H_2	44.53	30.36	26.23	28.33	26.14	28.24 (31.6)[a]
p5 + H	44.50	98.28	108.83	96.36	110.39	97.91
p6 + H_2	43.87	33.23	37.73	36.50	36.85	35.62
p7 + H_2	43.19	76.49	79.16	73.60	79.76	74.20
p8 + H_2	41.92	85.19	91.19	88.28	90.92	88.01
CH_3 + H_2CCCH	44.24	73.52	85.28	76.11	86.97	77.80 (77.0)[a]
CH_4 + H_2CCC	47.36	72.11	77.50	71.12	79.08	72.71 (76.3)[a]
CCH_2 + C_2H_4	46.64	70.80	70.06	68.57	77.42	75.93 (71.0)[a]
C_2H_3 + C_2H_3	45.60	98.12	114.90	98.94	117.11	101.14 (103.2)[a]

[a] In parenthesis: relative energy with respect to buta-1,2-diene based on experimental heats of formation from Ref. [39]. [b] The energy is calculated at the MRCI + Q(8,8)/6-311G** level (see "Decomposition of buta-1,3-diene" for the detailed discussion). [c] The G2M energy is computed using the MRCI + Q(8,8)/6-311G** energy instead of CCSD(T)/6-311G** (see "Decomposition of buta-1,3-diene").

46.6 kcal mol^{-1} and an energy loss of 43.0 kcal mol^{-1}. The barrier to and the heat of reaction for the H loss in but-1-yn-3-yl leading to vinylacetylene are calculated as 47.4 and 42.3 kcal mol^{-1}. Since the overall available energies for the but-2-yn-1-yl, buta-1,2-dien-4-yl, and but-1-yn-3-yl products after primary photodissociation of the parent buta-1,2-diene molecule at 193 nm are 63.4, 61.2, and 60.7 kcal mol^{-1}, the maximal translational energy they can have in order to be able to overcome the barriers on the secondary decomposition pathways is 7.7, 14.6, or 13.3 kcal mol^{-1}, respectively. This finding is in good agreement with the observation of the 7 kcal mol^{-1} cut-off in the translation energy distribution of the C_4H_5 products in the work of Neumark and co-workers.[21] The vinylacetylene + H products are expected to dominate the secondary decomposition of the C_4H_5 isomers, since the formation of C_2H_3 + C_2H_2 has to be preceded by isomerization of buta-1,2-dien-4-yl to buta-1,3-dien-4-yl over a barrier of 58.4 kcal mol^{-1}.

The only channel leading from buta-1,2-diene to molecular products in one step is the pathway producing CH_4 + H_2CCC (vinylidenecarbene). The reaction occurs via TS1 by a 1,2-H migration from the secondary CH group to the methyl fragment accompanied with cleavage of the C–C bond. The calculated barrier and the reaction heat are 83.6 and 72.7 kcal mol^{-1}, respectively. The latter value underestimates by 3.6 kcal mol^{-1} the experimental ΔH_r of 76.3 kcal mol^{-1}.[39] The transition state has a late and somewhat asynchronous character; the C–C bond in TS1 is practically broken but the migrating hydrogen is still closer to the former CH group carbon (1.18 Å) than to the methyl C atom (1.39 Å).

The other two channels resulting in molecular products occur by two-step mechanisms. For instance, vinylacetylene

Table 2. Harmonic vibrational frequencies (cm^{-1}) of various intermediates and transition states in photodissociation of buta-1,2-diene, buta-1,3-diene, and but-2-yne calculated at the B3LYP/6–311G** level.

Species	Frequencies [cm^{-1}]
buta-1,2-diene	68, 211, 340, 541, 572, 872, 879, 897, 1022, 1060, 1091, 1150, 1361, 1408, 1472, 1486, 1505, 2057, 3019, 3065, 3104, 3111, 3120, 3181
buta-1,3-diene	175, 300, 519, 539, 781, 899, 935, 936, 1001, 1004, 1058, 1227, 1315, 1320, 1415, 1473, 1653, 1706, 3123, 3132, 3135, 3136, 3219, 3220
but-2-yne	5, 201, 201, 383, 383, 725, 1054, 1054, 1057, 1057, 1171, 1417, 1420, 1482, 1482, 1482, 1482, 2366, 3020, 3020, 3075, 3075, 3076, 3076
i1	118, 165, 303, 435, 629, 825, 894, 976, 1018, 1049, 1099, 1200, 1313, 1340, 1411, 1428, 1491, 1608, 2921, 2990, 3006, 3063, 3129, 3230
i1′	76, 153, 235, 414, 567, 801, 834, 875, 972, 1003, 1035, 1216, 1288, 1377, 1447, 1451, 1474, 1506, 2948, 3004, 3011, 3057, 3146, 3244
i2	71, 154, 290, 333, 441, 576, 779, 825, 891, 1000, 1046, 1086, 1177, 1323, 1412, 1423, 1453, 1734, 2876, 3007, 3027, 3145, 3146, 3256
i3	154, 297, 323, 674, 737, 940, 975, 987, 1050, 1063, 1081, 1120, 1190, 1405, 1477, 1482, 1523, 1861, 3016, 3018, 3067, 3075, 3098, 3265
i4	136, 200, 226, 309, 391, 785, 973, 980, 1083, 1092, 1120, 1389, 1407, 1475, 1480, 1484, 1492, 1759, 3023, 3023, 3082, 3083, 3112, 3113
i5	323, 651, 866, 869, 887, 897, 941, 998, 1039, 1099, 1130, 1169, 1215, 1236, 1317, 1469, 1489, 1635, 3029, 3034, 3065, 3079, 3163, 3195
i6	83, 167, 253, 497, 546, 609, 769, 826, 885, 914, 1042, 1098, 1207, 1252, 1348, 1451, 1460, 1670, 2910, 3009, 3017, 3143, 3238, 3249
TS1	870i, 86, 156, 335, 385, 435, 607, 707, 773, 877, 989, 1034, 1148, 1166, 1430, 1441, 1469, 1986, 2408, 3062, 3117, 3193, 3196, 3248
TS2	580i, 151, 205, 422, 556, 603, 726, 824, 837, 990, 1069, 1115, 1221, 1379, 1445, 1459, 1497, 1842, 2393, 2989, 3049, 3095, 3163, 3255
TS3	1427i, 161, 319, 379, 595, 619, 716, 876, 902, 930, 954, 1000, 1088, 1221, 1299, 1377, 1443, 1600, 1701, 2646, 3125, 3138, 3224, 3276
TS4	746i, 148, 289, 465, 508, 623, 690, 694, 842, 905, 1012, 1078, 1197, 1296, 1375, 1444, 1474, 1750, 2781, 3014, 3089, 3120, 3160, 3273
TS5	158i, 32, 193, 311, 377, 512, 709, 809, 832, 949, 1002, 1038, 1238, 1284, 1362, 1474, 1637, 1657, 3073, 3135, 3161, 3215, 3240, 3249
TS6	1151i, 68, 306, 440, 598, 755, 892, 989, 1008, 1039, 1062, 1165, 1291, 1319, 1380, 1441, 1519, 1663, 2182, 2944, 3020, 3119, 3133, 3224
TS7	315i, 159, 346, 478, 594, 637, 711, 758, 830, 910, 999, 1088, 1219, 1272, 1402, 1431, 1518, 1680, 2700, 3051, 3130, 3139, 3157, 3257
TS8	2085i, 141, 256, 325, 491, 557, 768, 799, 839, 841, 895, 994, 1043, 1123, 1208, 1402, 1441, 1636, 1843, 1944, 3126, 3128, 3215, 3215
TS9	1069i, 106, 168, 263, 422, 566, 687, 812, 958, 1031, 1051, 1088, 1229, 1386, 1456, 1474, 1490, 1885, 2509, 2964, 3042, 3072, 3123, 3229
TS10	401i, 133, 254, 348, 691, 844, 888, 920, 961, 1041, 1068, 1188, 1352, 1367, 1444, 1491, 1512, 1527, 2946, 3041, 3052, 3074, 3098, 3272
TS11	908i, 170, 325, 346, 655, 823, 875, 1004, 1011, 1029, 1081, 1122, 1257, 1414, 1479, 1481, 1488, 1764, 2257, 3021, 3054, 3068, 3106, 3144
TS12	366i, 139, 169, 322, 324, 608, 897, 933, 960, 1055, 1072, 1330, 1412, 1455, 1474, 1488, 1492, 2002, 3019, 3025, 3079, 3106, 3122, 3187
TS13	500i, 174, 268, 358, 487, 500, 552, 674, 876, 932, 944, 1030, 1085, 1199, 1276, 1325, 1448, 1602, 1680, 3136, 3153, 3181, 3224, 3303
TS14	532i, 51, 154, 168, 382, 392, 507, 658, 766, 811, 961, 1031, 1054, 1120, 1275, 1403, 1453, 1485, 2166, 3008, 3051, 3062, 3068, 3465
TS15	627i, 266, 349, 422, 614, 651, 737, 799, 875, 899, 980, 1091, 1164, 1169, 1277, 1312, 1499, 1693, 2324, 3027, 3065, 3139, 3231, 3241
TS16	737i, 471, 650, 700, 743, 893, 899, 930, 957, 1013, 1031, 1123, 1165, 1245, 1385, 1512, 1519, 1544, 3070, 3071, 3141, 3161, 3205, 3206
TS17	92i, 177, 259, 506, 557, 613, 772, 833, 878, 920, 1046, 1092, 1211, 1249, 1342, 1453, 1463, 1666, 2918, 3017, 3023, 3143, 3235, 3249
TS18	383i, 298, 363, 448, 619, 639, 709, 749, 791, 935, 990, 1043, 1128, 1176, 1308, 1464, 1481, 1701, 2947, 3004, 3026, 3144, 3264, 3296
TSv1(2.4 Å)[a]	55, 185, 347, 409, 474, 665, 675, 773, 843, 870, 953, 1028, 1155, 1427, 1431, 1463, 2020, 3103, 3123, 3200, 3271, 3275, 3289
TSv2(2.2 Å)[a]	185, 218, 337, 457, 514, 638, 712, 824, 877, 1029, 1037, 1063, 1329, 1405, 1458, 1480, 1501, 2098, 3009, 3083, 3106, 3123, 3202
TSv3 [2.2 Å][a]	211, 321, 464, 545, 571, 683, 805, 880, 911, 935, 959, 994, 1114, 1191, 1374, 1459, 1496, 2007, 3101, 3134, 3170, 3176, 3277
TSv4 [2.4 Å][a]	146, 206, 390, 482, 558, 592, 634, 730, 786, 887, 1038, 1109, 1187, 1401, 1414, 1475, 1497, 2043, 3009, 3050, 3121, 3138, 3407
TSv5 [2.8 Å][a]	66, 115, 222, 295, 361, 749, 773, 852, 857, 926, 929, 976, 1024, 1378, 1381, 1598, 1656, 3051, 3052, 3152, 3157, 3242, 3249
TSv6 [2.4 Å][a]	170, 263, 327, 453, 502, 603, 631, 879, 889, 900, 968, 985, 1089, 1281, 1396, 1433, 1539, 1818, 3071, 3129, 3148, 3188, 3243
TSv7 [2.8 Å][a]	162, 224, 242, 317, 489, 589, 724, 820, 908, 936, 941, 1029, 1154, 1259, 1321, 1442, 1623, 1675, 3101, 3134, 3149, 3223, 3253
TSv8 [2.3 Å][a]	164, 202, 209, 382, 406, 509, 549, 771, 790, 1034, 1039, 1055, 1249, 1414, 1466, 1473, 1473, 2223, 3015, 3066, 3080, 3148, 3236

[a] Variational transition state calculated for the internal energy corresponding to photoexcitation by a 193 nm photon. In brackets: the reaction coordinate value.

$H_2CCHCCH$ (**p4**) and molecular hydrogen are produced via intermediate **i1**. The first step is 1,2-H migration from the CH group to the neighboring hydrogen-less carbon, overcoming a barrier of 62.8 kcal mol^{-1} at TS2. The intermediate **i1**, $H_2CCHCCH_3$, can be described as vinylmethylcarbene and resides 53.7 kcal mol^{-1} above buta-1,2-diene. We found two different structures of **i1**, which correspond to closed shell (carbene) and open shell (biradical) singlet electronic wave functions. In the biradical structure (**i1′** in Figure 1), the bonding within the carbon chain can be described as $H_2C^{\bullet}$-CH=C$^{\bullet}$-CH_3, while the carbene structure (**i1**) is characterized by the H_2C=CH-C:-CH_3 electronic configuration. Correspondingly, the CCC bond angles in **i1′**, 125.7° and 130.7°, are larger than those in **i1**, 117.3° and 114.1°. The calculated energies of the two electronic configurations at their optimized geometries are similar; **i1′** is more favorable than **i1** by 3.4 and 0.6 kcal mol^{-1} at the UB3LYP and UCCSD(T) levels,

0947-6539/03/0903-0732 $ 20.00+.50/0 *Chem. Eur. J.* **2003**, *9*, No. 3

respectively, but **i1** is preferred at the UMP2 level. At the final G2M level, **i1** resides 0.6 kcal mol^{-1} below the biradical structure. At the next step, H_2 elimination from the methyl group of **i1** yields vinylacetylene via transition state TS3. Thermodynamically, $H_2CCHCCH$ (**p4**) + H_2 are the most favorable products of the fragmentation of buta-1,2-diene, because this channel is endothermic by only 28.2 kcal mol^{-1} (ca. 31.6 kcal mol^{-1} in experiment).[39] However, the barriers for the H_2 loss are calculated to be high, 35.9 and 89.6 kcal mol^{-1} relative to **i1** and buta-1,2-diene, respectively. It is worth noting that the H_2 elimination barrier from vinylmethylcarbene is quite similar to that from methylcarbene, 34.1 kcal mol^{-1} at a similar CCSD(T)/6-311 + G(3df,2p)//B3LYP/6-311G** level of theory.[42]

An alternative two-step decomposition channel starts with 1,2-hydrogen migration from the methyl group of buta-1,2-diene via TS4. The H shift leads to a biradical intermediate **i2**, $H_2C^{\bullet}$-CH_2-$C^{\bullet}$=CH_2. The barrier at TS4, 72.0 kcal mol^{-1}, is ~10 kcal mol^{-1} higher than that at TS2, and **i2** lies 12.6 kcal mol^{-1} above **i1**. Next, the middle single C–C bond in **i2** can be cleaved leading to the ethylene plus vinylidene (CCH_2) products. The barrier at the corresponding transition state TS5 is 72.4 kcal mol^{-1} relative to buta-1,2-diene, but the reverse barrier for the vinylidene addition to ethylene is low, 2.4 or 3.6 kcal mol^{-1} at the B3LYP or CCSD(T) level, respectively. Note that the G2M scheme fails for CCH_2 + C_2H_4 and gives their energy higher than that for TS5 because of the large difference between the MP2/6-311 + G(3df,2p) and MP2/6-311G** energies for vinylidene (Table 1). The B3LYP/6-311G**- and CCSD(T)/6-311G**-calculated energies of CCH_2 + C_2H_4, 70.8 and 68.6 kcal mol^{-1}, respectively, are close to the value of 71.0 based on the best estimate of the relative energy of vinylidene with respect to acetylene[43] and experimental heats of formation for C_2H_2 and C_2H_4.[39] It is well known that CCH_2 can easily isomerize to acetylene, overcoming a 1.3 kcal mol^{-1} barrier with an energy gain of ~43 kcal mol^{-1}.[43] We tried to find a transition state directly connecting the $H_2CCH_2CCH_2$ intermediate with the more favorable ethylene + acetylene products. However, the TS search always converged to TS5 connected to CCH_2 + C_2H_4. Although a first-order saddle point on PES for the direct **i2** → C_2H_2 + C_2H_4 process apparently does not exist, one cannot exclude that some higher-energy trajectories involving H migration in conjunction with C–C bond cleavage may lead to acetylene and ethylene. On the other hand, since the C_2H_2 + C_2H_4 translational-energy distribution measured for the buta-1,2-diene photodissociation peaks at about 15–20 kcal mol^{-1}, these products should have a significant amount of internal energy, and the CCH_2 primary product is expected to rapidly isomerize to acetylene.

Buta-1,2-diene → buta-1,3-diene isomerization: The intermediates **i1** and **i2** are also involved in the isomerization of buta-1,2-diene to buta-1,3-diene. The G2M-calculated isomerization energy is −11.9 kcal mol^{-1}, in close agreement with the experimental value of −12.8 kcal mol^{-1}.[39] A 1,2-H shift from the methyl group in **i1** leads to buta-1,3-diene via TS6, with a barrier of 8.3 kcal mol^{-1}. Both barriers on the buta-1,2-diene → TS2 → **i1** → TS6 → buta-1,3-diene pathway have similar heights relative to the initial reactant, 62.8 and 62.0 kcal mol^{-1}. 1,2-H migration from the middle CH_2 group to the next hydrogen-less carbon in **i2** also leads to buta-1,3-diene. The 1,2-butadine → TS4 → **i2** → TS7 → buta-1,3-diene pathway is less favorable than the isomerization channel involving **i1** because the barriers at TS4 and TS7 relative to buta-1,2-diene are higher, 72.0 and 74.7 kcal mol^{-1}, respectively. **i2** could decompose to CH_2 + H_2CCCH_2 (allene) through cleavage of the CH_2–CH_2 bond. Based on the experimental ΔH_f for CH_2 and allene[39] and the calculated relative energy of **i2**, the bond cleavage is exothermic by 44.7 kcal mol^{-1} for the spin-allowed process leading to the singlet carbene and by 35.7 for the spin-forbidden fragmentation giving triplet CH_2. These energies are significantly higher than the barriers on the pathways from **i2** to buta-1,3-diene and CCH_2 + C_2H_4, and CH_2 + allene are unlikely to be produced.

Buta-1,2-diene → but-2-yne isomerization: The **i1** intermediate is also a precursor for the formation of but-2-yne. This process can occur by a 1,2-H shift from the CH group to CH_2 via TS9. However, the calculated barriers are high, 24.8 and 78.9 kcal mol^{-1} relative to **i1** and buta-1,2-diene, respectively, and an alternative multistep mechanism is preferable. The first stage of this mechanism is a ring closure in **i1** to produce the 1-methylcyclopropene intermediate (**i3**) overcoming a low 2.9 kcal mol^{-1} barrier at TS10. TS10 is an early transition state with the forming C–C bond as long as 2.080 Å. This is in accord with the high exothermicity of the **i1** → **i3** rearrangement calculated as 35.0 kcal mol^{-1}. 1-Methylcyclopropene resides 18.7 kcal mol^{-1} higher in energy than buta-1,2-diene. The next isomerization step is 1,2-H migration from the CH to CH_2 group in the tricarbon cycle accompanied by cleavage of the C–C bond and leading to ring opening. This process occurs via transition state TS11; the calculated barriers are 37.8 and 56.5 kcal mol^{-1} with regards to 1-methylcyclopropene and buta-1,2-diene, respectively. The H migration/ring opening leads to another intermediate **i4**, dimethylvinylidene, which is 45.0 kcal mol^{-1} less stable than buta-1,2-diene. The third and final isomerization step involves 1,2 migration of a CH_3 group via TS12; this can also be described as intramolecular insertion of the carbene carbon atom of dimethylvinylidene into a C–C bond. This rearrangement produces but-2-yne through a barrier of 10.6 kcal mol^{-1}. It is worth noting that this barrier is much higher than the barrier for the H migration in vinylidene producing acetylene, for which the best estimate is 1.3 kcal mol^{-1}.[43] Therefore, dimethylvinylidene is expected to be significantly more kinetically stable than vinylidene. Overall, buta-1,2-diene isomerizes to but-2-yne by the following four-step mechanism: buta-1,2-diene → TS2 (62.8 kcal mol^{-1}) → **i1** (53.7) → TS10 (56.6) → **i3** (18.7) → TS11 (56.5) → **i4** (45.0) → TS12 (55.6) → but-2-yne, and the highest barrier is calculated for the first step. At the G2M level, but-2-yne is 3.5 kcal mol^{-1} more stable than buta-1,2-diene; this agrees with the experimental energy difference of 4.1 kcal mol^{-1}.[39]

During photodissociation of buta-1,2- and -1,3-dienes or but-2-yne, the **i3** and **i4** intermediates are not likely to undergo direct dissociation through a cleavage of C–H or

  0947-6539/03/0903-0733 $ 20.00+.50/0

single C–C bonds because this would lead to high-lying isomers of C_4H_5 (+ H) and C_3H_3 (+ CH_3). For instance, methyl-group elimination from 1-methylcyclopropene would form a cyclic C_3H_3 structure and CH_3 loss from dimethylvinylidene would result in the $CCCH_3$ isomer. Both cyclic and linear isomers lie about 40 kcal mol^{-1} above the most stable H_2CCCH configuration.[44] Therefore, the C–C single-bond strengths in **i3** and **i4** can be estimated as 99.2 and 72.9 kcal mol^{-1}, and the overall reaction endothermicity starting from buta-1,2-diene is 117.9 kcal mol^{-1}; this makes these decomposition pathways less competitive.

Decomposition of buta-1,3-diene: Let us now turn to fragmentation channels of buta-1,3-diene not related to its isomerization to buta-1,2-diene. H elimination from a CH group gives buta-1,2-dien-4-yl (**p2**) with an energy loss of 98.8 kcal mol^{-1}. This reaction takes place with a break of C_s symmetry, so that the CCC angle at the carbon atom losing hydrogen eventually approaches 180°, and the neighboring CH_2 fragment rotates by 90°. H loss from a terminal CH_2 group gives another isomer of the C_4H_5 radical: *trans*,*trans*-buta-1,3-dien-4-yl (**p5**). According to our calculations, *trans*,-*trans*-$H_2CCHCHCH$ is 13.2 kcal mol^{-1} higher in energy than but-2-yn-1-yl; this is close to the CCSD(T) result of Parker and Cooksy of 12.3 kcal mol^{-1}.[40] The calculated heat of the buta-1,3-diene → *trans*,*trans*-$H_2CCHCHCH$ + H dissociation is 109.8 kcal mol^{-1}. Breaking the middle single C–C bond in buta-1,3-diene gives two vinyl radicals, C_2H_3 + C_2H_3, with an energy loss of 113.0 kcal mol^{-1}. At the G2M level, the C_2H_3 + C_2H_3 products lie 101.1 kcal mol^{-1} above buta-1,2-diene as compared with 103.2 kcal mol^{-1} obtained from experimental heats of formation.[39] Buta-1,3-diene can eliminate molecular hydrogen via TS8 producing butatriene (**p6**) with an endothermicity of 47.5 kcal mol^{-1}. However, the barrier for this process is high, 114.4 kcal mol^{-1} relative to buta-1,3-diene. Two hydrogen atoms are eliminated from the two middle carbons (four-center or 1,2-H_2 loss). On the reactant side, TS8 is connected to the *cis* isomer of buta-1,3-diene, which is 3.0 kcal mol^{-1} less stable than the *trans* isomer,[45] but the *trans* → *cis* isomerization requires a relatively low barrier of 5.6 kcal mol^{-1}[45] and should be facile for the energized molecule irradiated by 193 nm laser light. An alternative three-center (1,1-H_2) elimination from the terminal carbon atom of buta-1,3-diene is more favorable, although it leads to a high-lying isomer of the C_4H_4 species, vinylvinylidene $H_2CCHCHC$ (**p7**). **p7** is 46.0 and 38.6 kcal mol^{-1} less stable than vinylacetylene and butatriene, respectively, and can rearrange to the former by a 1,2-H shift over a low barrier of ~4 kcal mol^{-1}.[46] The energy loss in the buta-1,3-diene → **p7** + H_2 dissociation is 86.1 kcal mol^{-1}, and the reaction barrier occurs at TS13. The barrier heights in the forward and reverse directions, 96.0 and 9.9 kcal mol^{-1}, respectively, are quite similar to those for the 1,1-H_2 loss from ethylene of 93.9 and 11.8 kcal mol^{-1}.[42] The structure of the active CH_2 fragment in TS13 also closely resembles that of the corresponding transition state for the $C_2H_4 \rightarrow CCH_2 + H_2$ reaction,[42] although the former exhibits a slightly later character than the latter judging by the lengths of the breaking C–H and forming H–H bonds.

Two channels exist for buta-1,3-diene decomposition to acetylene and ethylene. The first one involves 1,3-hydrogen migration from the terminal CH_2 group via transition state TS15. The G2M-calculated energy of TS15 is 75.6 kcal mol^{-1} relative to buta-1,2-diene, so the barrier with respect to buta-1,3-diene is 87.5 kcal mol^{-1}. The products, C_2H_2 + C_2H_4, reside ~28 and ~40 kcal mol^{-1} above buta-1,2-diene and buta-1,3-diene, respectively. The structure of the transition state is peculiar; the 1,3-H shift is nearly completed in TS15, with forming and breaking C–H bond lengths of 1.177 and 2.022 Å, respectively. On the other hand, the breaking C–C single bond in the transition state is only slightly stretched to 1.529 Å as compared with 1.456 Å in the reactant. Also, the double C=C bond (1.337 Å in buta-1,3-diene), which is to become a triple bond in the acetylene product shortens to 1.295 Å in TS15. Thus, TS15 is an asynchronous transition state, and the decomposition process can be described as a 1,3-H shift before the barrier followed by C–C bond cleavage after the barrier is cleared. This conclusion is confirmed by the intrinsic reaction coordinate (IRC) calculations[47] of the minimal energy reaction path; these unambiguously show that TS15 indeed connects buta-1,3-diene with the C_2H_2 + C_2H_4 products. We also tried to find transition states for the similar two-step decomposition involving sequential 1,2-H migrations and replacing the 1,3-H shift via TS15. However, all our attempts to optimize saddle points for the 1,2-H shifts resulted in TS15; this indicates that in this case the 1,3-H shift is more favorable.

The second channel leading to acetylene + ethylene involves isomerization of *cis*-buta-1,3-diene to cyclobutene (**i5**). The buta-1,3-diene → cyclobutene rearrangement, which can occur through conrotatory and disrotatory pathways, has been studied before.[48, 49] The most accurate calculations at the CASSCF level were reported by Oliva et al.[49] who showed that the conrotatory pathway via a C_2-symmetric transition state is preferable. Our B3LYP calculations closely reproduce the CASSCF-optimized structure of the conrotatory transition state (see TS16 in Figure 3).[49] The barriers calculated at the G2M level are 42.3 and 32.7 kcal mol^{-1} relative to *cis*-buta-1,3-diene and cyclobutene, respectively. The latter value is fairly close to the 36.5 kcal mol^{-1} obtained by Oliva et al. at the CASSCF level.[49] According to our results, cyclobutene lies 0.7 and 12.6 kcal mol^{-1} higher in energy than buta-1,2-diene and *trans*-buta-1,3-diene, respectively; this is in reasonable agreement with the experimental values of −1.3 and 11.5 kcal mol^{-1}.[39] At the next reaction stage, cyclobutene can decompose to C_2H_2 + C_2H_4. The symmetric one-step fragmentation is a reverse reaction of the [2+2] cycloaddition and is forbidden according to the Woodward–Hoffmann rules. Nevertheless, Hess et al.[50] were able to find the C_2-symmetric transition state at the HF level with the STO-3G, 3-21G, and 6-31G* basis sets, and reported a barrier calculated at the MP2/6-31G*//HF/6-31G* level of 113 kcal mol^{-1} relative to cyclobutene. Hess et al. carried out vibrational frequency calculations at the HF/STO-3G and HF/3-21G levels and confirmed the transition state as a first-order saddle point within these approximations. We were able to reproduce the transition state structures reported by Hess et al.;[50] however, the HF/6-31G* calculations gave two

0947-6539/03/0903-0734 $ 20.00+.50/0 *Chem. Eur. J.* **2003**, *9*, No. 3

imaginary frequencies (second-order saddle-points). This is also the case in our B3LYP/6-311G** approximation; the transition state optimization within C_2 symmetry gives a second-order saddle point. When the symmetry was relaxed, we obtained an asymmetric transition state (TS18), which will be discussed in the next paragraph. Thus, the symmetric dissociation of cyclobutene to acetylene and ethylene is not favorable, and one has to consider another mechanism involving a biradical intermediate.

The asymmetric decomposition of cyclobutene **i5** starts from the cleavage of one of the single H_2C–CH bonds leading to the biradical species **i6** via TS17. The intermediate possesses the $H_2C^{\cdot}$-CH_2-CH=$CH^{\cdot}$ electronic configuration and lies 69.43 (68.73) kcal mol^{-1} higher in energy than buta-1,2-diene (cyclobutene). The structure of TS17 is very close to that of **i6**, and the transition state also exhibits an open-shell singlet character of the wavefunction. The relative energy of TS17 is only 0.02 kcal mol^{-1} higher than that of **i6**; this indicates that the latter is only a metastable intermediate. At the next step, **i6** can decompose to $C_2H_2 + C_2H_4$ by the cleavage of the longest (1.510 Å) C–C single bond via TS18. The reaction is highly exothermic, and the transition state depicts an early character, with the breaking bond stretched only by 4.6% to 1.580 Å. The energy of TS18 appeared to be very difficult to calculate. As seen in Table 1, its relative energies with respect to buta-1,2-diene obtained at the B3LYP/6-311G**, MP2/6-311G**, and MP2/6-311+G(3df,2p) levels with B3LYP/6-311G** *ZPE* corrections are 92.8, 89.5, and 88.3 kcal mol^{-1}, respectively. However, at the CCSD(T)/6-311G** level, the energy suddenly drops to 68.3 kcal mol^{-1}. This is apparently due to a failure of the perturbation theory in the treatment of triple substitutions (in the CCSD(T) method). Indeed, the CCSD/6-311G** energy of TS18 is 89.5 kcal mol^{-1}, in reasonable agreement with the B3LYP and MP2 values. For comparison, the quadratic configuration interaction[51] QCISD and QCISD(T) relative energies of TS18 with the same basis set are 86.7 and 73.4 kcal mol^{-1}; this also indicates that the perturbational treatment of triple substitutions is not adequate. Unfortunately, full variational CCSDT calculations of the C_4H_6 system are beyond our computational facilities. Therefore, we carried out multireference calculations of TS18 using the CASSCF method[52] with (14,14) active space as well as CASPT2[53] and MRCI[54] methods with (8,8) active space. The results, 79.2, 82.6, 81.9, and 85.1 kcal mol^{-1} at the CASSCF(14,14)/6-311G**, CASPT2(8,8)/6-311G**, MRCI(8,8)/6-311G**, and MRCI (with Davidson correction for quadruple excitations [MRCI + Q(8,8)/6-311G**]) levels, respectively, are in better agreement with the CCSD, QCISD, MP2, and B3LYP values than with those from the CCSD(T) and QCISD(T) calculations. Since the MRCI + Q result is expected to be the most accurate, we used it instead of the CCSD(T) value in the G2M scheme and obtained the final estimate of the relative energy of TS18 as 83.8 kcal mol^{-1} relative to buta-1,2-diene (see Table 1). Summarizing, the decomposition of cyclobutene to acetylene plus ethylene occurs by the following mechanism: **i5** → TS17 → **i6** → TS18 → $C_2H_2 + C_2H_4$, but since **i6** is only separated from **i5** by a tiny barrier of 0.02 kcal mol^{-1}, this process can be considered as a one-step (but asymmetric) dissociation, **i5** → TS18 → $C_2H_2 + C_2H_4$, with a barrier of 83.1 kcal mol^{-1} relative to cyclobutene.

Decomposition of but-2-yne: But-2-yne can isomerize to buta-1,2-diene or buta-1,3-diene via the **i1** intermediate and then undergo decomposition through the channels described above. In addition, one can think of three fragmentation pathways. First, H loss from a methyl group gives but-2-yn-1-yl with an endothermicity of 88.6 kcal mol^{-1}. Second, 1,1-H_2 elimination can take place from a CH_3 group resulting in the methylethynylcarbene isomer of C_4H_4 (**p8**), HCCCCH_3. This process is computed to be 91.5 kcal mol^{-1} endothermic and to proceed through a barrier of 98.9 kcal mol^{-1} at TS14. The reverse barrier for the H_2 addition to the carbene site of HCCCCH_3 is 7.4 kcal mol^{-1}, and the transition state exhibits a distinct late, product-like character. The H–H bond in TS14 is only 7% longer than this bond in free H_2, while two breaking C–H bonds elongate to 1.58 and 2.10 Å. Lastly, methyl group elimination by a cleavage of a single C–C bond produces CCCH_3, but this process is much less favorable. As was mentioned above, the CCCH_3 isomer of C_3H_3 is 40.1 kcal mol^{-1} less stable than the propargyl radical, H_2CCCH.[44] Using this value, we obtain the C–C bond strength in but-2-yne as 121.4 kcal mol^{-1}, which makes the direct CH_3 loss from but-2-yne uncompetitive compared with the other dissociation channels.

Reaction rate constants and product branching ratios: The kinetic scheme used for the calculation of product branching ratios is depicted in Figure 5. The RRKM-calculated rate constants are collected in Table 3 and the branching ratios are presented in Table 4. Figure 6 shows the plots of concentrations versus time for various intermediates and products in the photodissociation of buta-1,2-diene, buta-1,3-diene, and but-2-yne at 193 nm.

Dissociation of buta-1,2-diene: The $CH_3 + C_3H_3$ product channel clearly dominates photodissociation of buta-1,2-diene. Our calculations gave the branching ratio of these products as 87.9%. This is caused by the fact that the rate constant for the buta-1,2-diene → $CH_3 + C_3H_3$ dissociation, $k_{v1} = 5.13 \times 10^{10}$ s^{-1}, is more than an order of magnitude higher than the rates of isomerization of buta-1,2-diene to **i1**, $k_1 = 4.60 \times 10^9$ s^{-1}, and to **i2**, $k_2 = 2.46 \times 10^9$ s^{-1}, and almost two orders of magnitude higher than the rates of H-atom loss (k_{v2}, k_{v3}, k_{v4}) to produce the various C_4H_5 isomers. C_4H_5 is the second significant photodissociation product with but-2-yn-1-yl (**p1**), buta-1,2-dien-4-yl (**p2**), and but-1-yn-3-yl (**p3**) contributing 2.5%, 1.9%, and 1.3%, respectively. As **p3** is exclusively produced directly from buta-1,2-diene, small amounts of **p1** and **p2** arise from but-2-yne and buta-1,3-diene, respectively, after isomerization of buta-1,2-diene to these intermediates. The fourth isomer of C_4H_5, *trans*,*trans*-buta-1,3-dien-4-yl (**p5**), formed by H loss from buta-1,3-diene contributes only 0.16%. The total branching ratio of the C_4H_5 products is calculated as ~5.9%, so that the $CH_3 + C_3H_3$/C_4H_5 + H ratio is 87.9:5.9. This value is somewhat lower than the experimental value of 96:4.[21] However, in experiment a significant fraction of the C_4H_5 radicals possess a sufficient

  0947-6539/03/0903-0735 $ 20.00+.50/0

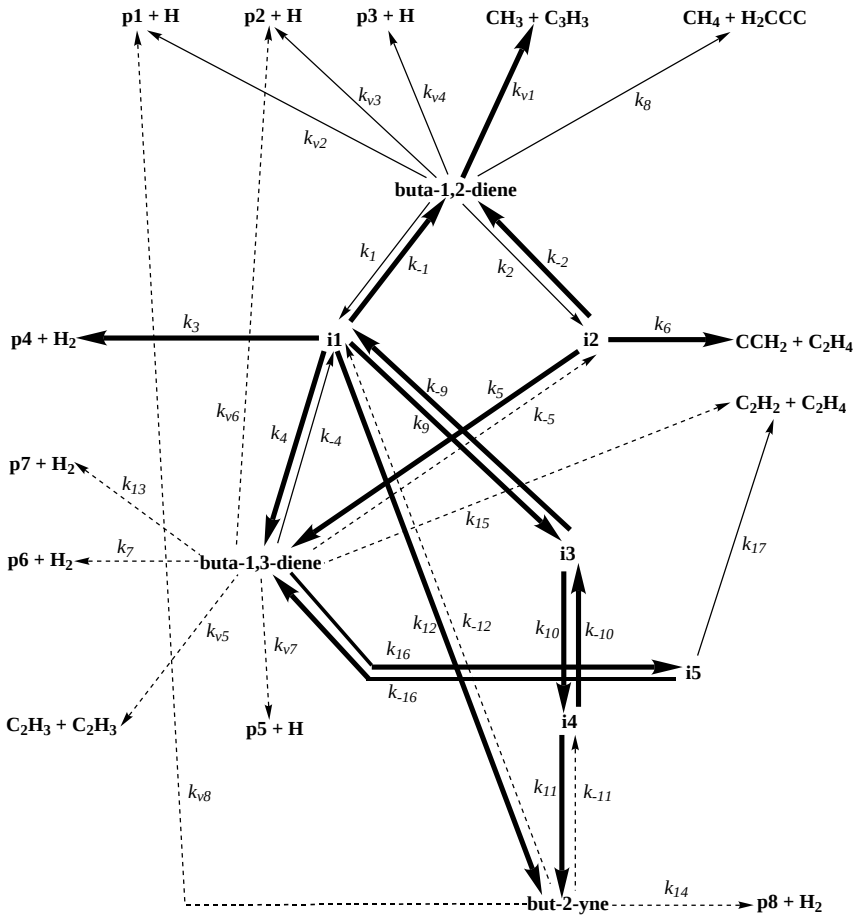

Figure 5. Reaction scheme used for kinetic modeling. Bold, thin, and dashed arrows correspond to rate constants higher than 10^{10}, between 5×10^8 and 10^{10}, and below 5×10^8 s^{-1}, respectively.

amount of internal energy to undergo secondary dissociation, mostly by a loss of another hydrogen atom (see "Decomposition of buta-1,2-diene"). Therefore, the agreement between theoretical and experimental results is satisfactory.

Possible molecular dissociation channels include $CH_4 + H_2CCC$ (1.1%, directly from buta-1,2-diene), $CCH_2 + C_2H_4$ (3.8%, via intermediate **i2**), $C_2H_2 + C_2H_4$ (0.3%, via buta-1,3-diene), and $C_4H_4 + H_2$ (totally about 0.5% but mostly (0.4%) vinylvinylidene (**p7**) through H_2 loss in buta-1,3-diene). These product channels as well as $C_2H_3 + C_2H_3$ play minor roles and were not detected in the experimental study of photodissociation of buta-1,2-diene at 193 nm.[21] We also note that the direct fragmentation of buta-1,2-diene is faster than its isomerization to buta-1,3-diene and but-2-yne. As seen in Figure 6a, the concentration of buta-1,3-diene reaches its maximum of about 4% at an early reaction stage before this minor amount decomposes into various products, while the maximum amount of but-2-yne, only ~1.5%, is achieved at about 0.5 ns. The concentrations of other intermediates along the reaction course are even lower. Summarizing, the major photodissociation products are formed from buta-1,2-diene in one step, while the formation of a number of minor products involves two or more isomerization steps.

Dissociation of buta-1,3-diene: Photodissociation of buta-1,3-diene is more versatile than photodissociation of buta-1,2-diene in terms of the products formed because of the competition between the buta-1,3-diene → buta-1,2-diene isomerization with other fragmentation pathways. The isomerization is a faster process since its rates, $k_{-1}k_{-4}/(k_4 + k_{-1}) = 6.17 \times 10^8$ via **i1** and $k_{-2}k_{-5}/(k_5 + k_{-2}) = 9.20 \times 10^7$ via **i2**, are higher than or comparable with the dissociation rates for buta-1,3-diene → **p2** + H, $k_{v6} = 9.80 \times 10^7$, buta-1,3-diene → $C_2H_3 + C_2H_3$, $k_{v5} = 4.92 \times 10^7$, buta-1,3-diene → **p5** + H, $k_{v7} = 1.31 \times 10^7$, buta-1,3-diene → $C_2H_2 + C_2H_4$ (by the 1,3-H shift via TS15), $k_{15} = 3.90 \times 10^7$, and the steady-state rate constants for the production of acetylene and ethylene via cyclobutene, $k_{17}k_{16}/(k_{-16} + k_{17}) = 8.41 \times 10^6$ (all rates are given in s^{-1}). As seen in Figure 6b, the concentration of the $CH_3 + C_3H_3$ products increases as that of buta-1,3-diene drops, and $CH_3 + C_3H_3$ formed by the C–C bond cleavage in buta-1,2-diene are again the major reaction products with a branching ratio of 49.6%. Interestingly, the concentration of buta-1,2-diene remains very small along the reaction course because it dissociates rapidly after being formed. The second important products are $C_4H_5 + H$. The buta-1,2-dien-4-yl isomer of C_4H_5, **p2**, is produced both directly from buta-1,3-diene and from buta-1,2-diene and contributes 9.7%. Interestingly, the calculated branching ratio of but-2-yn-1-yl (**p1**) is higher, 12.7%, although it cannot be produced directly from buta-1,3-diene. This fact illustrates the importance of the isomerization processes. In addition to the buta-1,3-diene → buta-1,2-diene rearrangement, buta-1,3-diene can also isomerize to but-2-yne via the **i1** intermediate. As seen in Figure 6b, the concentration of but-2-yne rises to about 20% before it isomerizes back or decomposes mostly to **p1** + H. The possibility of the formation of **p1** through two different isomerization pathways is responsible for its high branching ratio. The other two isomers of C_4H_5, *trans,trans*-buta-1,3-dien-4-yl (**p5**) formed directly from buta-1,3-diene and but-1-yn-3-yl (**p3**) produced via buta-1,2-diene, contribute only 1.2% and 0.4%, respectively. The branching ratio of the third radical product $C_2H_3 + C_2H_3$, which is formed by single C–C bond cleavage in buta-1,3-diene, amounts to 4.6%. Among the molecular channels, the most important is the formation of C_2H_2 (vinylidene or acetylene) and C_2H_4. The contribution of CCH_2 (vinylidene) + C_2H_4 produced via **i2** is 10.7%, and that of acetylene + ethylene formed by the other routes (see "Decomposition of buta-1,3-diene") is 4.5%. Finally, the H_2 elimination from

0947-6539/03/0903-0736 $ 20.00+.50/0 *Chem. Eur. J.* **2003**, *9*, No. 3

Table 3. RRKM-calculated unimolecular rate constants [s^{-1}], symmetry factors, and barrier heights [kcal mol^{-1}] of various reaction steps in the photodissociation of buta-1,2-diene, buta-1,3-diene, and but-2-yne at 193 nm.

Rate constant	buta-1,2-diene	buta-1,3-diene	but-2-yne	Symmetry factor	Barrier height
k_1	4.603×10^9	1.988×10^9	3.653×10^9	1	62.8
k_{-1}	2.871×10^{12}	2.348×10^{12}	2.718×10^{12}	1	9.1
k_2	2.463×10^9	8.648×10^8	1.846×10^9	3	72.0
k_{-2}	1.295×10^{12}	1.117×10^{12}	1.240×10^{12}	2	5.8
k_3	4.062×10^{10}	1.509×10^{10}	3.135×10^{10}	3	35.9
k_4	7.776×10^{12}	6.581×10^{12}	7.419×10^{12}	3	8.3
k_{-4}	5.860×10^9	2.346×10^9	4.562×10^9	2	73.9
k_5	4.552×10^{11}	3.708×10^{11}	4.308×10^{11}	2	8.5
k_{-5}	4.109×10^8	1.226×10^8	2.949×10^8	2	86.6
k_6	6.483×10^{12}	5.544×10^{12}	6.217×10^{12}	1	6.2
k_7	1.582×10^6	1.475×10^5	8.339×10^5	1	114.4
k_8	6.526×10^8	1.568×10^8	4.426×10^8	1	83.6
k_9	3.582×10^{12}	3.388×10^{12}	3.528×10^{12}	1	2.9
k_{-9}	1.144×10^{11}	6.729×10^{10}	9.880×10^{10}	1	37.9
k_{10}	8.206×10^{10}	4.763×10^{10}	7.005×10^{10}	1	37.8
k_{-10}	3.045×10^{12}	2.476×10^{12}	2.861×10^{12}	6	11.5
k_{11}	4.560×10^{12}	3.793×10^{12}	4.337×10^{12}	2	10.6
k_{-11}	3.528×10^8	1.745×10^8	2.903×10^8	2	59.1
k_{12}	4.280×10^{11}	2.370×10^{11}	3.614×10^{11}	1	24.8
k_{-12}	3.981×10^7	1.125×10^7	2.807×10^7	6	82.0
k_{13}	2.641×10^8	5.544×10^7	9.101×10^7	2	96.0
k_{14}	1.437×10^7	1.933×10^6	8.373×10^6	6	98.9
k_{15}	1.355×10^8	3.898×10^7	9.627×10^7	1	87.5
k_{16}	1.206×10^{10}	7.905×10^9	1.072×10^{10}	1	45.3
k_{-16}	4.240×10^{11}	3.151×10^{11}	4.007×10^{11}	1	32.7
k_{17}	1.350×10^9	3.356×10^8	9.238×10^8	2	83.1
k_{v1}	5.131×10^{10}	2.138×10^{10}	4.044×10^{10}	1	(63.2)[a]
k_{v2}	8.138×10^8	2.401×10^8	5.833×10^8	1	(76.8)[a]
k_{v3}	6.729×10^8	1.850×10^8	4.739×10^8	3	(79.1)[a]
k_{v4}	7.688×10^8	1.859×10^8	5.231×10^8	2	(82.7)[a]
k_{v5}	3.052×10^8	4.919×10^7	1.862×10^8	1	(103.0)[a]
k_{v6}	4.611×10^8	9.803×10^7	3.023×10^8	2	(95.2)[a]
k_{v7}	1.014×10^8	1.305×10^7	5.836×10^7	4	(107.1)[a]
k_{v8}	1.630×10^8	4.241×10^7	1.137×10^8	6	(81.7)[a]

[a] In parenthesis: relative energy of the variational transition state with respect to the reactant.

Table 4. Calculated product branching ratios [%] in the photodissociation of buta-1,2-diene, buta-1,3-diene, and but-2-yne at 193 nm.

Products	buta-1,2-diene	buta-1,3-diene	but-2-yne
p1 + H	2.53	12.7	56.6
p2 + H	1.86	9.67	4.34
p3 + H	1.32	0.43	0.31
p5 + H	0.16	1.23	0.78
$CH_3 + C_3H_3$	87.9	49.6	23.8
$CH_4 + C_3H_2$	1.12	0.36	0.26
p4 + H_2	0.06	0.36	0.32
p6 + H_2	0.0	0.01	0.01
p7 + H_2	0.41	5.22	1.22
p8 + H_2	0.10	0.55	4.15
$C_2H_3 + C_2H_3$	0.47	4.64	2.50
$CCH_2 + C_2H_4$	3.82	10.7	3.98
$C_2H_2 + C_2H_4$	0.27	4.47	1.62

buta-1,3-diene giving vinylvinylidene is also significant with the branching ratio of 5.2%.

Overall, we obtained the following product branching ratios for buta-1,3-diene photodissociation at 193 nm: C_4H_5 + H/CH_3 + C_3H_3/C_2H_3 + C_2H_3/C_4H_4 + H_2/C_2H_2 + C_2H_4 = 24.0:49.6:4.6:6.1:15.2. The corresponding experimental branching ratios are[22] 20:50:8:2:20 and one can see that the differences between the theoretical and experimental results do not exceed 5%. For the two molecular channels we can also compare our results with the experimental measurements for 1,1,4,4-[D_4]buta-1,3-diene. In the C_4H_4 + H_2 channel, Neumark and co-workers reported 9:27:64 branching ratios for H_2, HD, and D_2 loss, respectively.[22] Unless the D and H atoms are scrambled in 1,1,4,4-[D_4]buta-1,3-diene, the buta-1,3-diene → **p7** + H_2 channel gives D_2, buta-1,3-diene → **i1** → **p4** + H_2 produces ⅔ HD and ⅓ D_2, buta-1,3-diene → **p6** + H_2 gives H_2, and but-2-yne → **p8** + H_2 results in ⅔ HD and ⅓ D_2. Based on this, the H_2/HD/D_2 branching ratios can be computed as 0.2:9.9:89.9. The significant underestimation of the experimental branching ratios for H_2 and HD indicates that some isotope scrambling does occur. Such scrambling is possible through reversible isomerization of buta-1,3-diene to **i1**; this should increase the yield of HD, while the buta-1,3-diene → **i1** → buta-1,2-diene → **i2** → buta-1,3-diene → **i1** → buta-1,3-diene rearrangements can lead to the formation of the H_2 isotopomer through channels leading to **p4** and **p7**.

When the deuterated 1,1,4,4-[D_4]buta-1,3-diene species undergoes decomposition to the major molecular products, acetylene and ethylene, the buta-1,3-diene → **i2** → CCH_2 + C_2H_4 channel should give $C_2D_2H_2$, buta-1,3-diene → C_2H_2 + C_2H_4 (by the 1,3-H shift via TS15) should produce C_2D_3H, and buta-1,3-diene → **i5** (cyclobutene) → C_2H_2 + C_2H_4 yield C_2D_4. The experimental $C_2D_2H_2/C_2D_3H/C_2D_4$ branching ratios are 29:39:32,[22] but the calculated ratio between the three channels is 70.5:24.3:5.2. Such disagreement again indicates that the H/D isotope scrambling via intermediates **i1** and **i2** apparently takes place faster than the decomposition.

Dissociation of but-2-yne: The product branching ratios calculated for the photodissociation of but-2-yne at 193 nm are quite different from those obtained for buta-1,2- and -1,3-dienes. For instance, C_4H_5 + H are the major products, with the **p1** and **p2** isomers contributing 56.6% and 4.3%, respectively. On the other hand, the relative yield of the CH_3 + C_3H_3 radicals decreases to 23.8%. As for buta-1,3-diene, the direct (one-step) decomposition channels, but-2-yne → **p1** + H and but-2-yne → **p8** + H_2, compete with the isomerization of but-2-yne to buta-1,2- and -1,3-dienes. The hydrogen loss rate leading to but-2-yn-1-yl **p1**, $k_{v8} = 1.14 \times 10^8\ s^{-1}$, is slightly slower than the rate for the but-2-yne → **i4** rearrangement, $k_{-11} = 2.90 \times 10^8\ s^{-1}$, but is similar to the steady-state rate for the but-2-yne → **i4** → **i3** process, $k_{-10}k_{-11}/(k_{11} + k_{-10}) = 1.15 \times 10^8\ s^{-1}$. k_{v8} exceeds the rate for molecular hydrogen loss to produce **p8**, $k_{14} = 8.37 \times 10^6\ s^{-1}$, by more than an order of magnitude. The above consideration indicates that about a half of the products are formed directly from but-2-yne and the other half are produced through multiple isomerization steps. For instance, the CH_3 + C_3H_3 products and a significant fraction of C_4H_5 (**p1**) + H originate from the C–C and C–H bond cleavages in buta-1,2-diene, while **p2** + H (4.3%) are formed both from buta-1,2- and -1,3-dienes. The formation of other minor products also requires several rearrangements before dissociation.

The overall C_4H_5 + H/CH_3 + C_3H_3/C_2H_3 + C_2H_3/C_4H_4 + H_2/C_2H_2 + C_2H_4 branching ratio is calculated as

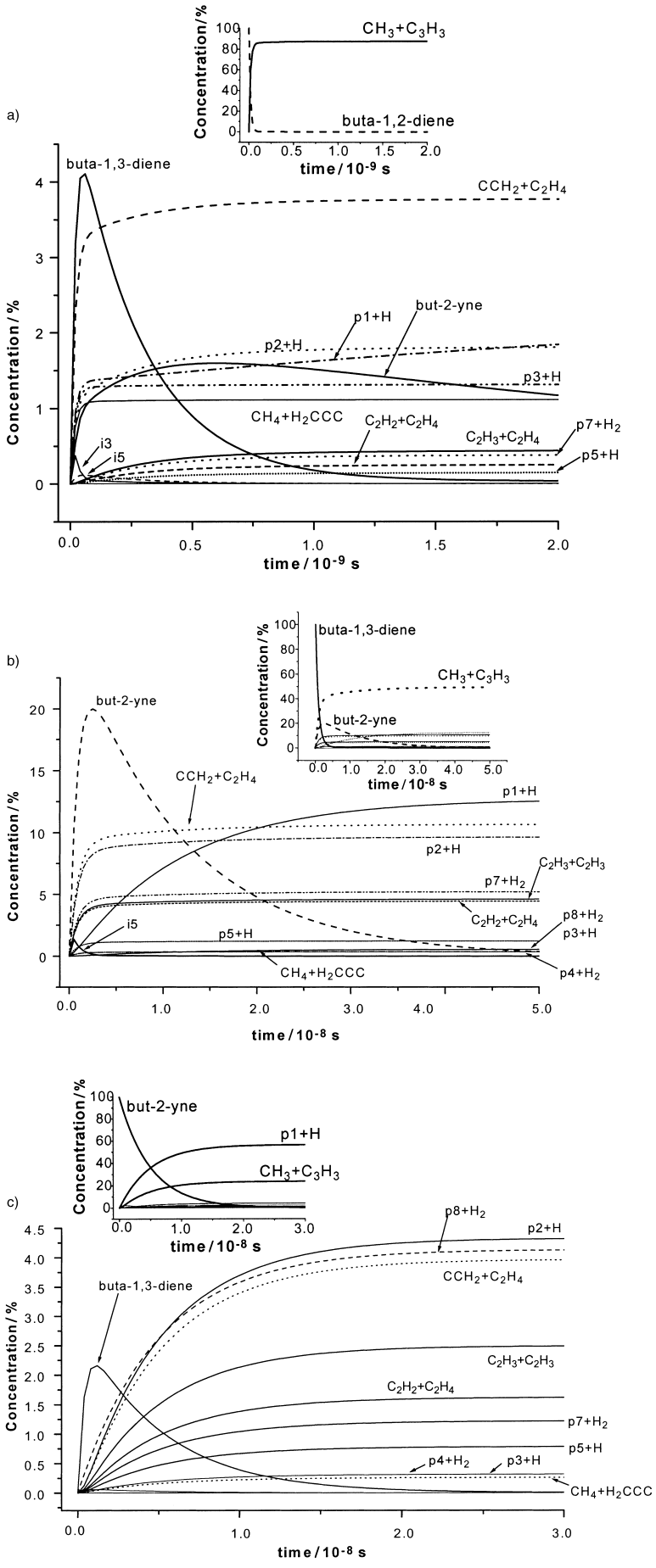

Figure 6. Calculated kinetic curves for photodissociation of a) buta-1,2-diene, b) buta-1,3-diene, and c) but-2-yne at 193 nm. The large plots show the products and intermediates with small concentrations, and the insets depict those with large concentrations.

62.0:23.8:2.5:5.7:5.6 with $CH_4 + H_2CCC$ contributing the remaining minor amount. No experimental measurements have been performed so far for but-2-yne photodissociation at 193 nm, but in terms of the accuracy of our results for buta-1,2- and -1,3-dienes we expect that the predicted relative yields should be trusted within 5% margins. But-2-yne is the only C_4H_6 isomer (among the three isomers considered here), for which photodissociation is expected to produce more hydrogen atoms than methyl radicals.

Conclusion

Ab initio G2M calculations have been carried out in order to understand the reaction mechanism of photodissociation of three isomers of the C_4H_6 molecule, buta-1,2- and -1,3-dienes, and but-2-yne after their internal conversion from an excited electronic state into the vibrationally excited ground electronic state. For buta-1,2-diene, the major dissociation channels are single C–C bond cleavage to form the methyl and propargyl radicals and loss of hydrogen atoms from various positions to produce the but-2-yn-1-yl (**p1**), buta-1,2-dien-4-yl (**p2**), and but-1-yn-3-yl (**p3**) isomers of C_4H_5. The minor channels include molecular dissociations to methane + vinylidenecarbene and vinylidene + ethylene. Ab initio calculations of the ground state PES were followed by microcanonical RRKM calculations of energy-dependent rate constants for individual reaction steps (under collision-free conditions) and by solution of kinetic equations aimed at predicting the relative product yields (branching ratios). The calculated branching ratio of the $CH_3 + C_3H_3/C_4H_5 + H$ products, 87.9:5.9, is in a good agreement with the recent experimental value of 96:4 measured by Neumark and co-workers,[21] taking into account that a significant amount of the C_4H_5 products undergo secondary dissociation to $C_4H_4 + H$. The isomerization of buta-1,2-diene to buta-1,3-diene or but-2-yne appears to be slower than its one-step decomposition and therefore plays only a minor role.

Photodissociation of buta-1,3-diene is shown to be a more intricate process, where the buta-1,3-diene → buta-1,2-diene, buta-1,3-diene → but-2-yne, and buta-1,3-diene → cyclobutene rearrangements play a significant role. The major reaction products are still $CH_3 + C_3H_3$, which are formed

0947-6539/03/0903-0738 $ 20.00+.50/0 *Chem. Eur. J.* **2003**, *9*, No. 3

after the isomerization of buta-1,3-diene to buta-1,2-diene. However, the contribution of the other radical channels, $C_4H_5 + H$ and $C_2H_3 + C_2H_3$, as well as two molecular channels, $C_2H_2 + C_2H_4$ and $C_4H_4 + H_2$, significantly increases. The overall theoretical $C_4H_5 + H/CH_3 + C_3H_3/C_2H_3 + C_2H_3/C_4H_4 + H_2/C_2H_2 + C_2H_4$ branching ratios are 24.0:49.6:4.6:6.1:15.2 and agree with the experimental relative yields[22] of 20:50:8:2:20 within the 5% margins. Again, considering that a fraction of the C_4H_5 products has sufficient internal energy to undergo a secondary H atom loss, the agreement between theory and experiment is even better. Two channels have been characterized for the buta-1,3-diene → buta-1,2-diene rearrangement both involving two sequential 1,2-hydrogen migrations. The first mechanism proceeds via the intermediate **i1** (vinylmethylcarbene) and exhibits highest barriers of 74.7 and 62.8 kcal mol^{-1} relative to 1,3- and buta-1,2-dienes, respectively. The second pathway passes through the biradical intermediate **i2** and depicts the highest barriers of 86.6 and 74.7 kcal mol^{-1} in the forward and reverse directions. The $C_4H_4 + H_2$ products are formed mostly through the three-center molecular hydrogen loss in buta-1,3-diene that gives the vinylvinylidene isomer of the C_4H_4 molecule. Three channels leading to the C_2H_2 products have been found, of which the most significant one involves the 1,2-H migration from one CH group in buta-1,3-diene to the other followed by C–C bond cleavage (via **i2**). The second channel is the 1,3-H migration from CH_2 to CH accompanied by C–C bond cleavage, and the third and least-important channel involves rearrangement of *trans*-buta-1,3-diene to its *cis* conformation, four-member ring closure through a conrotatory pathway producing cyclobutene followed by asymmetric decomposition of the latter into $C_2H_2 + C_2H_4$.

For but-2-yne, the direct (one-step) decomposition pathways mostly including H atom loss producing **p1** and, to a lesser extent, molecular hydrogen elimination yielding **p8** play an approximately even role with that of the channels involving the isomerization of but-2-yne to 1,2- or buta-1,3-dienes. As a result, **p1** + H become the most important reaction products with a branching ratio of 56.6% followed by $CH_3 + C_3H_3$ (23.8%). The overall $C_4H_5 + H/CH_3 + C_3H_3/C_2H_3 + C_2H_3/C_4H_4 + H_2/C_2H_2 + C_2H_4$ branching ratio is predicted as 62.0:23.8:2.5:5.7:5.6. Thus, contrary to buta-1,2- and -1,3-dienes, photodissociation of but-2-yne is expected to produce more hydrogen atoms than methyl radicals. The isomerization mechanism of but-2-yne to buta-1,2- and -1,3-dienes has been shown to proceed through several steps and to involve the dimethylvinylidene (**i4**), 1-methylcyclopropene (**i3**), and **i1** intermediates. The highest barriers calculated along the isomerization pathways from but-2-yne to buta-1,2-diene and buta-1,3-diene are 66.3 and 65.5 kcal mol^{-1}, respectively, in the forward direction and 62.8 and 73.9 kcal mol^{-1} in the reverse direction.

Acknowledgement

This work was supported in part by Academia Sinica and the National Science Council of Taiwan, R.O.C. under Grant NSC 91-2113-M-001-029.

[1] R. Schinke, *Photodissociation Dynamics*, University Press, Cambridge, **1993**.
[2] J. Collin, F. P. Lossing, *Can. J. Chem.* **1957**, *35*, 778.
[3] R. D. Doepker, K. L. Hill, *J. Phys. Chem.* **1969**, *73*, 1313.
[4] Z. Diaz, R. D. Doepker, *J. Phys. Chem.* **1977**, *81*, 1442.
[5] R. Srinivasan, *Adv. Photochem.* **1966**, *4*, 113.
[6] I. Haller, R. Srinivasan, *J. Chem. Phys.* **1964**, *40*, 1992.
[7] I. Haller, R. Srinivasan, *J. Am. Chem. Soc.* **1966**, *88*, 3694.
[8] R. D. Doepker, *J. Phys. Chem.* **1968**, *72*, 4037.
[9] G. J. Collin, H. Deslauriers, G. R. D. Maré, R. A. Poirer, *J. Phys. Chem.* **1990**, *94*, 134.
[10] L. Letendre, D. K. Liu, C. D. Pibel, J. B. Halpern, H. L. Dai, *J. Chem. Phys.* **2000**, *112*, 9209.
[11] B. K. Venkataraman, J. J. Valentini, *Chem. Phys. Lett.* **1992**, *194*, 191.
[12] C. H. Wu, R. D. Kern, *J. Phys. Chem.* **1987**, *91*, 6291.
[13] R. D. Kern, H. J. Singh, C. H. Wu, *Int. J. Chem. Kinet.* **1988**, *20*, 731.
[14] Y. Hidaka, T. Higashihara, N. Ninomiya, T. Oki, H. Kawano, *Int. J. Chem. Kinet.* **1995**, *27*, 331.
[15] G. B. Skinner, E. M. Sokoloski, *J. Phys. Chem.* **1960**, *64*, 1028.
[16] J. H. Kiefer, K. I. Mitchell, H. C. Wei, *Int. J. Chem. Kinet.* **1988**, *20*, 787.
[17] J. H. Kiefer, H. C. Wei, R. D. Kern, *Int. J. Chem. Kinet.* **1985**, *17*, 225.
[18] J. H. Kiefer, S. S. Kumaran, P. S. Mudipalli, *Chem. Phys. Lett.* **1994**, *224*, 51.
[19] V. S. Rao, G. B. Takeda, G. B. Skinner, *Int. J. Chem. Kinet.* **1988**, *20*, 153.
[20] Y. Hidaka, T. Higashihara, N. Ninomiya, H. Masaoka, T. Nakamura, H. Kawano, *Int. J. Chem. Kinet.* **1996**, *28*, 137.
[21] J. C. Robinson, W. Sun, S. A. Harris, F. Qi, D. N. Neumark, *J. Chem. Phys.* **2001**, *115*, 8359.
[22] J. C. Robinson, S. A. Harris, W. Sun, N. E. Sveum, D. N. Neumark, *J. Am. Chem. Soc.* **2002**, *124*, 10211.
[23] W. L. Feng, M. Lei, Y. Wang, Y. Qian, *Chin. Chem. Lett.* **1997**, *8*, 71.
[24] Y. Wang, W. L. Feng, M. Lei, R. Z. Liu, *Sci. China Ser. B: Chem.* **1998**, *41*, 60.
[25] M. Lei, Y. Qian, Y. Wang, W. L. Feng, *Chem. J. Chin. Univ. (Chinese)* **1998**, *19*, 586.
[26] A. D. Becke, *J. Chem. Phys.* **1993**, *98*, 5648.
[27] C. Lee, W. Yang, R. G. Parr, *Phys. Rev. B* **1988**, *37*, 785.
[28] A. M. Mebel, K. Morokuma, M. C. Lin, *J. Chem. Phys.* **1995**, *103*, 7414.
[29] L. A. Curtiss, K. Raghavachari, G. W. Trucks, J. A. Pople, *J. Chem. Phys.* **1991**, *94*, 7221.
[30] J. A. Pople, M. Head-Gordon, D. J. Fox, K. Raghavachari, L. A. Curtiss, *J. Chem. Phys.* **1989**, *90*, 5622.
[31] L. A. Curtiss, C. Jones, G. W. Trucks, K. Raghavachari, J. A. Pople, *J. Chem. Phys.* **1990**, *93*, 2537.
[32] L. A. Curtiss, K. Raghavachari, J. A. Pople, *J. Chem. Phys.* **1993**, *98*, 5523.
[33] G. D. Purvis, R. J. Bartlett, *J. Chem. Phys.* **1982**, *76*, 1910.
[34] Gaussian 98 (Revision A.7), M. J. Frisch, G. W. Trucks, H. B. Schlegel, G. E. Scuseria, M. A. Robb, J. R. Cheeseman, V. G. Zakrzewski, J. A. Montgomery, R. E. Stratmann, J. C. Burant, S. Dapprich, J. M. Millam, A. D. Daniels, K. N. Kudin, M. C. Strain, O. Farkas, J. Tomasi, V. Barone, M. Cossi, R. Cammi, B. Mennucci, C. Pomelli, C. Adamo, S. Clifford, J. Ochterski, G. A. Petersson, P. Y. Ayala, Q. Cui, K. Morokuma, D. K. Malick, A. D. Rabuck, K. Raghavachari, J. B. Foresman, J. Cioslowski, J. V. Ortiz, B. B. Stefanov, G. Liu, A. Liashenko, P. Piskorz, I. Komaromi, R. Gomperts, R. L. Martin, D. J. Fox, T. Keith, M. A. Al-Laham, C. Y. Peng, A. Nanayakkara, C. Gonzalez, M. Challacombe, P. M. W. Gill, B. G. Johnson, W. Chen, M. W. Wong, J. L. Andres, M. Head-Gordon, E. S. Replogle, J. A. Pople, Gaussian, Inc., Pittsburgh, PA, **1998**.
[35] MOLPRO is a package of ab initio programs written by H.-J. Werner and P. J. Knowles with contributions from J. Almlöf, R. D. Amos, M. J. O. Deegan, S. T. Elbert, C. Hampel, W. Meyer, K. Peterson, R. Pitzer, A. J. Stone, P. R. Taylor, R. Lindh.
[36] J. I. Steinfeld, J. S. Francisco, W. L. Hase, *Chemical Kinetics and Dynamics*, Prentice-Hall, Englewood Cliffs, NJ, **1999**.
[37] H. Eyring, S. H. Lin, S. M. Lin, *Basic Chemical Kinetics*, Wiley, New York, **1980**.
[38] P. J. Robinson, K. A. Holbrook, *Unimolecular Reactions*, Wiley, New York, **1972**.

  0947-6539/03/0903-0739 $ 20.00+.50/0

[39] *NIST Chemistry Webbook*, NIST Standard Reference DataBase Number 69- February **2000** Release (http://webbook.nist.gov/chemistry/).
[40] a) C. L. Parker, A. L. Cooksy, *J. Phys. Chem. A* **1998**, *102*, 6186; b) C. L. Parker, A. L. Cooksy, *J. Phys. Chem. A* **1999**, *103*, 2160.
[41] T. L. Nguyen, A. M. Mebel, R. I. Kaiser, unpublished results.
[42] a) A. H. H. Chang, A. M. Mebel, X.-M. Yang, S. H. Lin, Y. T. Lee, *Chem. Phys. Lett.* **1998**, *287*, 301; b) A. H. H. Chang, A. M. Mebel, X.-M. Yang, S. H. Lin, Y. T. Lee, *J. Chem. Phys.* **1998**, *109*, 2748.
[43] N.-Y. Chang, C.-H. Shen, C.-H. Yu, *J. Chem. Phys.* **1997**, *106*, 3237.
[44] a) T. L. Nguyen, A. M. Mebel, R. I. Kaiser, *J. Phys. Chem. A* **2001**, *105*, 3284; b) T. L. Nguyen, A. M. Mebel, S. H. Lin, R. I. Kaiser, *J. Phys. Chem. A* **2001**, *105*, 11549.
[45] I. Handorf, H. Y. Lee, A. M. Mebel, S. H. Lin, Y. T. Lee, R. I. Kaiser, *J. Chem. Phys.* **2000**, *113*, 9622.
[46] A. M. Mebel, M. C. Lin, D. Chakraborty, J. Park, S. H. Lin, Y. T. Lee, *J. Chem. Phys.* **2001**, *114*, 8421.
[47] C. Gonzalez, H. B. Schlegel, *J. Phys. Chem.* **1990**, *94*, 5523.
[48] a) J. Breulet, H. F. Schaefer III, *J. Am. Chem. Soc.* **1984**, *106*, 1221; b) M. J. S. Dewar, R. C. Dougherty, *The PMO Theory of Organic Chemistry*, Plenum, New York, **1975**, pp. 343–346; c) H. E. Zimmerman, *Pericyclic Reactions, Vol. 1* (Eds.: A. P. Marchand, R. E. Lehr), Academic Press, New York, **1977**, pp. 53–107; d) K. N. Houk, *Pericyclic Reactions, Vol. 1* (Eds.: A. P. Marchand, R. E. Lehr), Academic Press, New York, **1977**, pp. 181–271; e) J. J. Gajewski, *Hydrocarbon Thermal Isomerizations*, Academic Press, New York, **1981**, pp. 47–50; f) L. Salem, *Electrons in Chemical Reactions: First Principles*, Wiley, New York, **1982**, pp. 130–132 and 163–164; g) K. Hsu, R. J. Buenker, S. D. Peyerimhoff, *J. Am. Chem. Soc.* **1971**, *93*, 2117; K. Hsu, R. J. Buenker, S. D. Peyerimhoff, *J. Am. Chem. Soc.* **1972**, *94*, 5639; h) M. J. S. Dewar, S. Kirschner, *J. Am. Chem. Soc.* **1974**, *96*, 6809; i) W. Thiel, *J. Am. Chem. Soc.* **1981**, *103*, 1420; j) L. Deng, T. Zigler, *J. Phys. Chem.* **1995**, *99*, 929.
[49] J. M. Oliva, J. Gerratt, P. B. Karadakov, D. L. Cooper, *J. Chem. Phys.* **1997**, *107*, 8917.
[50] B. Andes Hess, Jr., L. J. Schaad, D. N. Reinhoudt, *Int. J. Quantum Chem.* **1986**, *29*, 345.
[51] J. A. Pople, M. Head-Gordon, K. Raghavachari, *J. Chem. Phys.* **1987**, *87*, 5968.
[52] a) H.-J. Werner, P. J. Knowles, *J. Chem. Phys.* **1985**, *82*, 5053; b) P. J. Knowles, H.-J. Werner, *Chem. Phys. Lett.* **1985**, *115*, 259.
[53] H.-J. Werner, *Mol. Phys.* **1996**, *89*, 645.
[54] a) H.-J. Werner, P. J. Knowles, *J. Chem. Phys.* **1988**, *89*, 5803; b) P. J. Knowles, H.-J. Werner, *Chem. Phys. Lett.* **1988**, *145*, 514.

Received: June 27, 2002 [F4209]

  0947-6539/03/0903-0740 $ 20.00+.50/0